AGU100 ADVANCING EARTH AND SPACE SCIENCE

Space Weather

RESEARCH ARTICLE
10.1029/2018SW002105

Key Points:
- Relative robustness of the GPS L2C and L5 signals with legacy L1C/A signal in terms of cycle slips
- Correlation of intensity of amplitude scintillation with duration of cycle slip at L1C/A, L2C, and L5 frequency of GPS
- Comparative study of loss of lock over three frequencies of GPS above ICAO mentioned standards (6 s) from Calcutta

Correspondence to:
T. Biswas,
trisani77@gmail.com

Citation:
Biswas, T., Ghosh, S., Paul, A., & Sarkar, S. (2019). Interfrequency performance characterizations of GPS during signal outages from an anomaly crest location. *Space Weather*, *17*, 803–815. https://doi.org/10.1029/2018SW002105

Received 18 OCT 2018
Accepted 14 APR 2019
Accepted article online 4 MAY 2019
Published online 7 JUN 2019

Interfrequency Performance Characterizations of GPS During Signal Outages From an Anomaly Crest Location

T. Biswas[1], S. Ghosh[1], A. Paul[1], and S. Sarkar[1]

[1]Institute of Radio Physics and Electronics, University of Calcutta, Kolkata, India

Abstract Introduction of new navigation signals L2C (1227.60 MHz) and L5 (1176.45 MHz) to the existing GPS (Global Positioning System) spectrum, under the modernization program of GPS offers the improvement of position accuracy. The present study aims to understand the relative robustness of the L2C and L5 signals compared to legacy L1 C/A signal during periods of scintillations in terms of durations of cycle slips encountered from an anomaly crest location, Calcutta (22.58°N, 88.38°E geographic; magnetic dip 32°N). The data analyzed in this study were recorded during the vernal equinox of 2014 (February–April), a period of high solar activity of cycle 24. Results obtained from the comparative analyses, which are perhaps one of the first from the Indian longitude sector, indicate GPS L5 to be more robust than L1 C/A and L2C in terms of occurrence and duration of cycle slips under adverse ionospheric conditions. Furthermore, loss-of-lock events of duration greater than 6 s are found to be more frequent for $S_4 \geq 0.6$. It is found that frequency sensitivity of the GPS spectrum, in terms of occurrence of cycle slips and loss of locks are in conformity with earlier results from the equatorial region but are different from the high latitudes with respect to local time of occurrence and geomagnetic activity.

1. Introduction

The equatorial ionosphere is characterized by generation of intense irregularities in electron density distribution, particularly during the postsunset hours of equinoctial months, leading to formation of field aligned plasma bubbles in the *F* region of the ionosphere (Aarons, 1982; Anderson & Haerendel, 1979). Global Navigation Satellite System (GNSS) signals traversing through these irregularities can be distorted and may experience intense amplitude and phase fluctuations, referred to as scintillations. Such adverse conditions may sometimes disrupt satellite-Earth communication and navigation systems leading to complete outage of signals. This issue has drawn considerable attention of scientific as well as practical user community over many years.

Over the last decade, signals from GNSS have been strongly exploited to monitor and characterize the ionosphere and related dynamics concerned with scintillations of transionospheric radio signals. The diurnal and day-to-day variabilities of the equatorial ionosphere and particularly the Equatorial Ionization Anomaly (EIA) is a phenomenon well studied in literature (Basu et al., 2009; Bhattacharyya et al., 2003; Kelley et al., 1976; McClure et al., 1977; Paul & DasGupta, 2010; Rastogi & Klobuchar, 1990). Vilà-Valls et al. (2017) have presented a new model-based method to achieve a solution toward mitigation challenges posed by scintillation-corrupted measurements. Suggested techniques for improvement of satellite signal reception capability may apply the principles of spatial diversity of different satellite constellations (Paul et al., 2017), frequency diversity between different frequencies of GNSS satellite links (Goswami et al., 2017) and interoperability between different satellite-based navigation systems (Goswami et al., 2018).

The equatorial and low-latitude region is the seat of some of the most dynamic ionospheric characteristics in terms of ionization density or total electron content (TEC) and ionization density irregularities. Transionospheric satellite signal outages and resulting impact on satellite-based communication and navigation services from this region form the benchmark for the international Space Weather program with regard to its intensity, rapidity of fluctuations, and randomness of occurrence. The location of the present observing station at Calcutta situated near the northern crest of the EIA in the Indian longitude sector ensures that the most severe degradations in performance are encountered from this location during the equinoctial months under adverse ionospheric Space Weather conditions, which in this case, may not necessarily be associated with geomagnetic disturbed conditions. Similar statistics may emerge from the Brazilian sector as well where however such signal fadings normally occur during local summer months.

In the midlatitudes and the polar regions, such deterioration in satellite-based systems and services are usually correlated with geomagnetic disturbed conditions.

GPS (Global Positioning System) modernization program has introduced two new navigation signals L2C (1227.60 MHz) and L5 (1176.45 MHz) to the GPS constellation. The L2C signal will be dedicated for civilian applications, and it is expected to replace the semicodeless L2P(Y) signal. The L5 signal is exclusively reserved for aviation navigation services and is designed with a protected spectrum, higher power, and greater bandwidth to support life-critical and high-performance applications. Measurement of carrier phase of the transionospheric signal is essential for high precision measurement delivered by satellite-based navigation particularly for high dynamic platforms such as aircrafts (RTCA, 2006). Communication receivers are usually equipped with a dynamical range of signal fading, typically 25–30 dB-Hz, exceeding which the receiver fails to track the signal (Moraes et al., 2011; Seo et al., 2009). Therefore, fluctuation in phase introduced by the medium of propagation of the signal may lead to shift in frequency of the phase-locked loop (PLL), and when this shift exceeds certain bandwidth of the PLL, the receiver experiences loss of phase lock. Loss of lock occurs when the phase error exceeds a certain threshold of the PLL that causes the carrier frequency of the signal to fall outside the loop's frequency pull-in range (Humphreys et al., 2005, 2010). A PLL's phase detector being periodic is unable to distinguish between a phase error and integral multiple of it. Therefore, cycle slip is encountered when the phase error shifts in the order of $n \cdot 2\pi$, n being an integer. The fades introduced in the signal may cause cycle slips, which in turn may affect the receiver to encounter loss of lock on transmitted signals.

Roy and Paul (2013) have previously reported results on loss of lock of carrier tracking loop during the equinoctial months of 2011 by recording received phase of GPS L1 signal from two stations, Calcutta and Siliguri, separated by 4° of subionospheric latitude near the northern crest of EIA in the Indian longitude sector. Jiao et al. (2015) have characterized signal fading across triple frequency of GPS in terms of fading duration, time separation between fades and fading overlap in an attempt to improve interfrequency aiding algorithms in signal tracking. Deep power fade (>15 dB) induced by abrupt phase transition, especially in the equatorial region, is a subject well addressed by Humphreys et al. (2005, 2010). Relative motion between the satellite and the drifting ionospheric irregularities may lead to greater possibility of cycle slips (DasGupta et al., 2006; Kintner et al., 2001, 2004). A new algorithm used by Liu (2010) detects cycle slips from TEC rate, where the data are recorded at a sampling frequency of 1.0 Hz. The effectiveness of the algorithm works well for data recorded at high carrier frequency compared to cases of low carrier frequency where small cycle slips may sometimes be difficult to detect. Jiao et al. (2018) have simulated amplitude and phase scintillation data to study the effect of dynamics of the receiver platform on scintillation characteristics, and in turn, compare these effects for dynamic and stationary platforms.

Inverse dependence of occurrence of ionospheric scintillation on carrier frequency of signal is a well-known phenomenon. The relative performance of the different GPS frequencies, namely, L1, L2C, and L5 in terms of signal outages during periods of ionospheric scintillations could be interesting as well as valuable for system designers in their pursuit for assessing the signal strengths associated with the different GPS signals. Moraes et al. (2017) have reported studies of amplitude and phase scintillations on GPS triple frequency signals from São José dos Campos (23.1°S, 45.8°W; dip latitude 17.3°S, declination 21.4°W) located in Brazil, which shows that phase and amplitude scintillation are well correlated but the strength of the correlation increases toward cases of large intensities of scintillation. They have also found the loss of phase lock to be more frequent when the signal path becomes closer to the magnetic field lines. Intensity, duration, and occurrence frequency of scintillation have been studied by Jiao and Morton (2015) using multifrequency GPS scintillation data from high-latitude and equatorial stations. Effects of ionospheric scintillation on Global Navigation Satellite System (GLONASS) is presented by Moraes, Muella, et al. (2018), where L2 signal of the system is found to be 2 or 3 times more prone toward scintillation effects than L1. Additionally, this work has also compared GLONASS with GPS in terms of ionospheric scintillation effects and showed that constellation with fewer tracked satellites are more susceptible toward the effect.

The present study aims to analyze and compare the modernized GPS L2C and L5 signals with legacy L1 C/A signal in terms of occurrence and duration of cycle slips of the signals from Calcutta (22.58°N, 88.38°E geographic; magnetic dip 32°N), located near the northern crest of the EIA during the vernal equinoctial months of 2014. An attempt has been made to correlate S_4 with cycle slip duration, which would help in

10.1029/2018SW002105

understanding the impact of scintillation on the system performance. Comparative performances of the GPS triple frequency, during periods of signal outage could be essential information that has not been extensively reported from Indian longitude sector.

2. Data and Methodology

The present study has been done by utilizing data, obtained from a multifrequency, multiconstellation GNSS receiver (Septentrio PolaRxS Pro), operated at the Institute of Radio Physics and Electronics, University of Calcutta (22.58°N, 88.38°E geographic; magnetic dip 32°N) since 2013. This station being located in a geophysically sensitive region, transionospheric satellite signals are often disrupted by intense scintillations generated over the magnetic equator, especially during the postsunset hours of equinoctial periods (Paul et al., 2011). Hence, the signal outages from this location form an important benchmark for the international Space Weather program. Ray and DasGupta (2007) and Das et al. (2010) had observed the occurrence of post sunset GPS L band scintillation from Calcutta to be maximum during the equinoctial periods. This GNSS receiver is able to track and log data from GPS, GLONASS, and Galileo, as well as different Satellite-based Augmentation System satellites at corresponding transmission frequencies. GPS links are tracked by the receiver at three frequencies L1 (1575.42 MHz), L2 (1227.6 MHz), and L5 (1176.45 MHz). Some of the important output parameters logged by the receiver at a sampling rate of 50 Hz (0.02 s) are Coordinated Universal Time, carrier phase (cycle) of the received signal, carrier-to-noise ratio (C/N_O), and receiver position. Elevation, azimuth, TEC, amplitude scintillation index (S_4), and other related ionospheric parameters are recorded at sampling interval of 1 min.

The present analyses have been done under magnetically quiet conditions (with *Dst* index ≤ −50 nT) of the vernal equinoctial period of 2014 (February–April), which was a high solar activity period (monthly Smoothed Sunspot Number [SSN]: 146.1, 128.7, 112.5; F10.7: 147.9–188.1 SFU, 134.2–162.5 SFU, 119.6–185.2 SFU). Intense amplitude scintillations ($S_4 \geq 0.6$) were observed at GPS L1 frequency on 60 nights during February to April 2014 from Calcutta.

February:	10 nights
March:	31 nights
April:	19 nights

It is also important to mention that during March 2014, intense nighttime amplitude scintillation were observed at GPS L band from Calcutta on all 31 days. However, GPS L5 frequency being introduced under the GPS modernization program was transmitted by a significantly less number of satellites (SVID: 1, 24, 25, and 27) in 2014. A list of the number of satellites tracked by the 18-channel GNSS receiver at GPS L2C and L5 in 2014 is presented below.

Frequency	No. of SV links	SVIDs
(i) L2C	10	1, 5, 7, 12, 15, 24, 25, 27, 29, 31
(ii) L5	4	1, 24, 25, 27

In the present paper, while comparing GPS L1 C/A, L2C, and L5, only those cases have been considered when scintillations were observed at L1, L2C, and L5 on the same SV link, that is, SV1 and SV24 in 2014. During February–April 2014, number of nights during which intense amplitude scintillation were observed in all three GPS L band frequencies (L1, L2, and L5) are as follows:

February:	1, 18, 24, 26–28
March:	1–12, 14–17, 19, 22–27
April:	3, 6, 10

An elevation masking of 15° was maintained at all times while analyzing the data to minimize errors arising out of multipath effects.

Measurement of cycle slips are performed from the carrier phase of the received signals from GPS satellites transmitting L1, L2C, and L5 frequencies, recorded at 50-Hz sampling rate (0.02 s). The received phase data from the satellites consist of dominant contribution due to geometric path length and minor contributions from the ionosphere and Doppler effects. This received phase information is detrended by successive differencing to remove contributions from the geometrical path length and free-space Doppler and extract the ionospheric contribution (Hofmann-Wellenhof et al., 2008). A 90-min moving average of C/N_O has been calculated and thereafter subtracted from instantaneous C/N_O values to calculate deviations, if any. This process helps eliminate the slow variation of the signal arising out of satellite movements.

Outage of satellite signals refer to nonavailability of signals that are not attributable to hardware failure or poor satellite-to-receiver geometry. These discontinuities in the received signal as highlighted in the present paper are exclusively due to geophysical perturbations, caused by intersection of satellite signals with drifting ionospheric irregularities.

In an effort to compare GPS L1 C/A, L2C, and L5 frequencies in terms of signal outages in adverse ionospheric conditions, initially, this study has been performed independently on GPS L1 C/A, L2C, and L5 frequencies for all available satellites during March 2014. The objective behind this exercise was to demonstrate the magnitude of occurrence of loss of lock on each GPS frequency individually, considering all SVs together. The complete picture of the individual analysis on GPS L1 C/A, L2C, and L5 has been presented. Thereafter, comparative results of GPS L1 C/A, L2C, and L5 over the entire vernal equinoctial period of 2014 have been presented considering only SV 1 and SV 24.

In this context, it is important to indicate that the major objective of the present study is to exhibit the results of comparative analysis of GPS triple-frequency (L1 C/A, L2C, and L5) regime, on the basis of loss of lock of signal leading to cycle slips. In this process of representation, a case study for 18 February 2014 has been highlighted and statistical results for the entire equinoctial period have been presented.

3. Results

During the vernal equinox of 2014, sixty nights of intense ionospheric scintillations ($S_4 \geq 0.6$) were observed on GPS L band. Scattering of transionospheric satellite signals may take place as a result of intersection of signals with ionospheric irregularity structures causing intense ionospheric scintillations. Different studies on scattering of transionospheric signals have previously been reported in literature (Carrano et al., 2012; Singleton, 1970). This study essentially investigates the performance and robustness of the GPS triple-frequency (L1 C/A, L2C, and L5) signals during adverse ionospheric conditions.

Figures 1a and 1b show a representative case of maximum cycle slip detected at GPS L1 C/A on 26 March 2014, during 21:00–22:00 LT for a particular SV link (SV7) and corresponding C/N_O deviation during the same time interval. The second difference on received phase of the signal has been plotted in Figure 1b during 20:00–21:00 LT. From Figure 1b, a clear break in the received phase of the signal could be observed indicating loss of lock of 302.34 s starting around 21:54 LT. Figures 1d and 1e represent the respective C/N_O deviation and corresponding maximum loss of lock obtained at GPS L2C on 26 March 2014 on SV 7 during the same time interval of 21:00–22:00 LT. From Figure 1e, a loss of lock for 315.81 s can be measured on SV7 link at GPS L2C starting at 21:54 LT. The lock time of the signal, followed by the event of loss of lock was 31 s for L1 C/A and 29 s for L2C. Carrano and Groves (2010) have reported in a study that time of reacquisition of a signal after loss of lock event was 13.5 s on an average 50% of time. Since, SV7 was not equipped with transmitting L5 in 2014, in order to present a case of maximum cycle slip duration at L5, Figures 1g and 1h show the representative C/N_O deviation and corresponding second difference on phase at GPS L5 on the same day (26 March 2014) as observed in SV24. It shows that loss of lock encountered at GPS L5 is 1.66 s. However, over the entire period of analyses, maximum value of cycle slip duration at GPS L5 was found to be 2.54 s on SV24 on 3 April 2014. Figures 1c, 1f, and 1i present an enlarged section of the phase plot of Figures 1b, 1e, and 1h, respectively. It is important to note at this point that these values of cycle slips obtained for GPS L1 C/A and L2C on 26 March 2014 are in excess of that specified by International Civil Aviation Organization (ICAO) for Aeronautical Approach with Vertical Guidance (APV), namely, 6 s for APV-I and 10 s for APV-II, respectively, thereby resulting in possible hazards toward safety of civil aviation operations (International Civil Aviation Organization, 2006).

While comparing the triple-frequency GPS links in terms of loss of lock, detailed analyses have been performed for each frequency of GPS for the month of March 2014. A statistical description of the result of

10.1029/2018SW002105

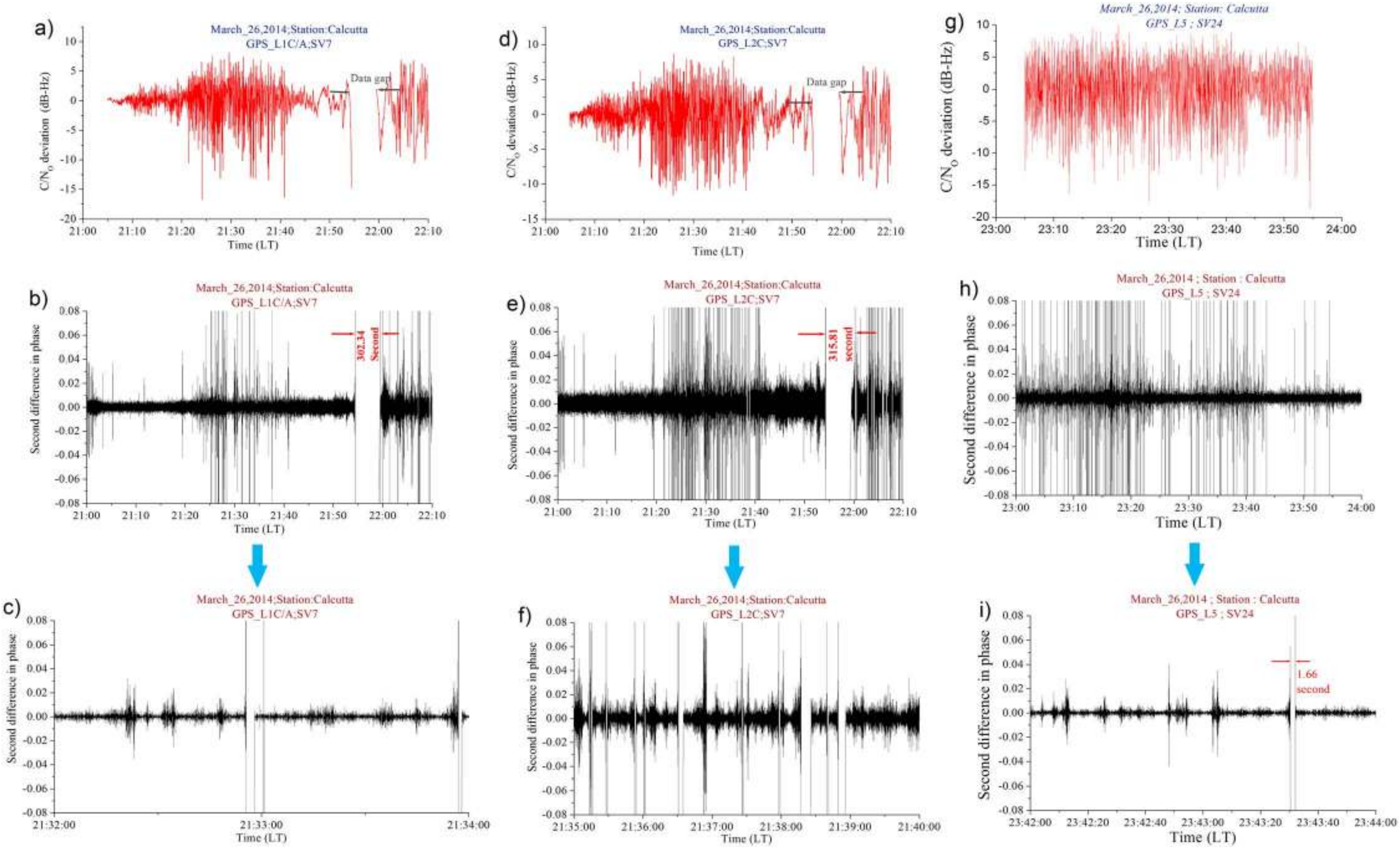

Figure 1. A representative case of maximum cycle slips encountered at GPS L1 C/A, L2C, and L5 on 26 March 2014. (a) C/N_O deviation at L1 C/A on SV7 during 21–22 LT. (b) Second difference in phase (cycles) at L1 C/A on SV7 during 21–22 LT. (c) Magnified version of second difference in phase (cycles) at L1 C/A on SV7 as observed in Figure 1b. (d) C/N_O deviation at L2C on SV7 during 21–22 LT. (e) Second difference in phase (cycles) at L2C on SV7 during 21–22 LT. (f) Magnified version of second difference in phase (cycles) at L2C on SV7 as observed in Figure 1e. (g) C/N_O deviation at L5 on SV24 during 23–24 LT. (h) Second difference in phase (cycles) at L5 on SV24 during 23–24 LT. (i) Magnified version of second difference in phase (cycles) at L5 on SV24 as observed in Figure 1h. GPS = Global Positioning System.

analyses is presented in Figure 2a where number of cases of cycle slips has been plotted in logarithmic scale as a function of different time durations for all GPS SV links at L1 C/A with elevation greater than 15°. From the figure, it is clear that although approximately 1,500 cases of cycle slips have been encountered having duration of 1–2 s, but there are also 85 cases of loss of lock measured for duration of 6–8 s and 24 cases when loss of lock was between 10 and 20 s. Further, six cases have been encountered when loss of lock was more than 60 s. In this regard, Table 1 shows the entire list of cycle slips encountered at GPS L1 C/A in terms of percentage of occurrence for different postsunset hours and its relation with intense scintillation during March 2014. Similarly, Figures 2b and 2c show the statistical description of loss of lock durations in logarithmic scale on GPS L2C and L5, respectively, during March 2014. From these plots, it could be observed that for L2C, 104 cases of loss of lock of duration 6–8 s have been noted and for duration of 10–20 s, 65 such cases are found. One thousand five hundred thirty-nine cases of loss of lock were detected at L2C, which are of duration 1–2 s. In case of GPS L5, loss of locks encountered were 102 cases of 1–2 s duration and only one case of 2–4 s duration. No cycle slip of longer duration is observed for GPS L5 during March 2014. Figure 2d depicts the overall distribution of cycle slips combining the statistics of L1 C/A, L2C, and L5 during March 2014, as obtained from Calcutta on all GPS SV links. In this context, it is important to note that, being introduced under the GPS modernization program, in March 2014, even though the number of SV links that transmitted GPS L2C was less, loss of locks of duration 6 s and more is found to be more frequent for L2C than L1 C/A during the period of analyses.

In an effort to correlate number of cases of cycle slip with intensity of amplitude scintillations, durations of cycle slip have been plotted with respect to amplitude scintillation index (S_4) in Figure 3. Considering cases

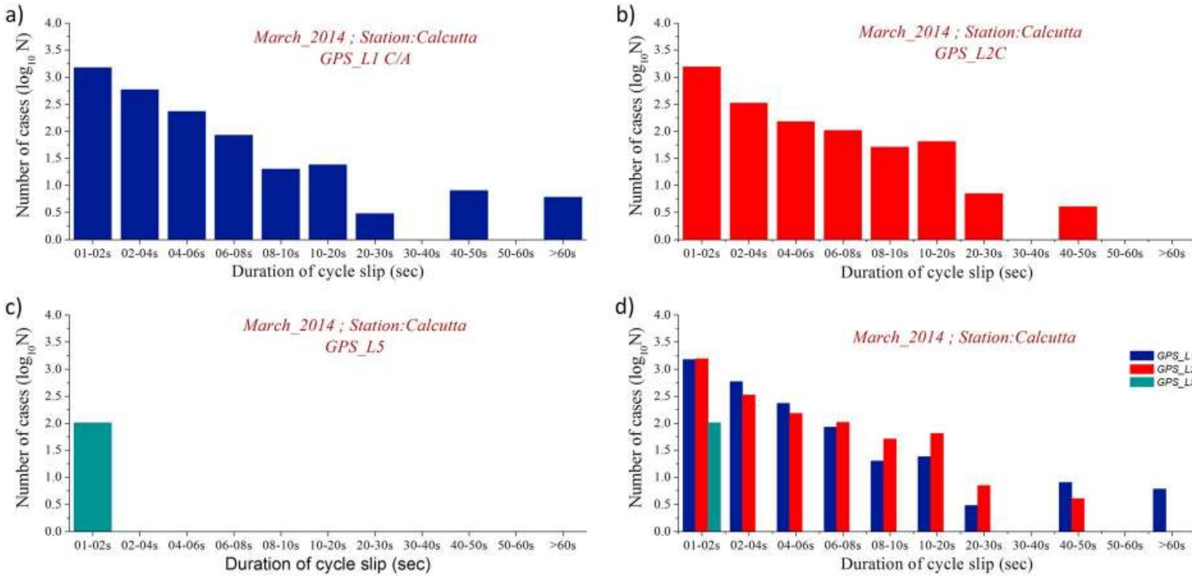

Figure 2. Statistical representation of cycle slips in logarithmic scale, observed at triple frequency of GPS during March 2014 from Calcutta. (a) Number of cases of cycle slips encountered at L1 C/A as a function of different time duration. (b) Number of cases of cycle slips encountered at L2C as a function of different time duration. (c) Number of cases of cycle slips encountered at L5 as a function of different time duration. (d) Comparative study between number of cases of cycle slips encountered respectively at L1 C/A, L2C, and L5 as a function of different time duration. GPS = Global Positioning System.

from all available GPS SV links at L1 C/A and L2C during March 2014, Figures 3a and 3b respectively show that cases of cycle slips are found to be more corresponding to S_4 values greater than 0.6, which is in accordance with Moraes et al. (2011). In order to clearly indicate this feature, a vertical red line has been drawn for $S_4 = 0.6$ and a similar horizontal line has also been drawn for loss of lock duration equal to 6 s. From the position of the horizontal line in Figures 3a and 3b, it is clear that majority of cycle slips greater than 6 s could be found for S_4 values greater than 0.6. Carrano and Groves (2010) have presented a case in their work that shows, for a particular S_4 value, rate of fading can be different for different satellites. Figure 3c shows the variation of S_4 with duration of cycle slip at GPS L5 where the red dotted line at $S_4 = 0.6$ marks the threshold for intense amplitude scintillations.

Table 1
Statistical Description of Loss of Lock Events Observed at GPS L1 C/A During March 2014 From Calcutta

Statistical description of loss of lock events observed at GPS L1 C/A March 2014
Station: Calcutta

Number of satellites tracked	Total number of loss of lock events encountered	Duration of the event	Percentage of occurrence of the event	Percentage of cases with $S_4 \geq 0.6$	Hourly values of occurrence of the event						
					19–20 LT	20–21 LT	21–22 LT	22–23 LT	23–00 LT	00–01 LT	01–02 LT
32	2,473	01–02 s	60.70%	45.61%	1.62%	13.91%	17.39%	11.48%	13.18%	2.18%	0.93%
		02–04 s	23.90%	16.86%	0.57%	4.08%	5.70%	4.33%	7.84%	1.09%	0.28%
		04–06 s	9.50%	8.90%	0.08%	1.33%	2.79%	1.86%	2.75%	0.61%	0.08%
		06–08 s	3.44%	3.44%	0%	0.28%	0.90%	0.65%	1.25%	0.28%	0.08%
		08–10 s	0.81%	0.77%	0%	0.08%	0.32%	0.16%	0.04%	0.20%	0%
		10–20 s	0.97%	0.97%	0%	0.04%	0.28%	0.44%	0.12%	0%	0.08%
		20–30 s	0.12%	0.08%	0%	0%	0%	0.12%	0%	0%	0%
		40–50 s	0.32%	0.32%	0%	0%	0%	0%	0.32%	0%	0%
		>60 s	0.24%	0.16%	0.04%	0.04%	0.08%	0.08%	0%	0%	0%

Note. GPS = Global Positioning System.

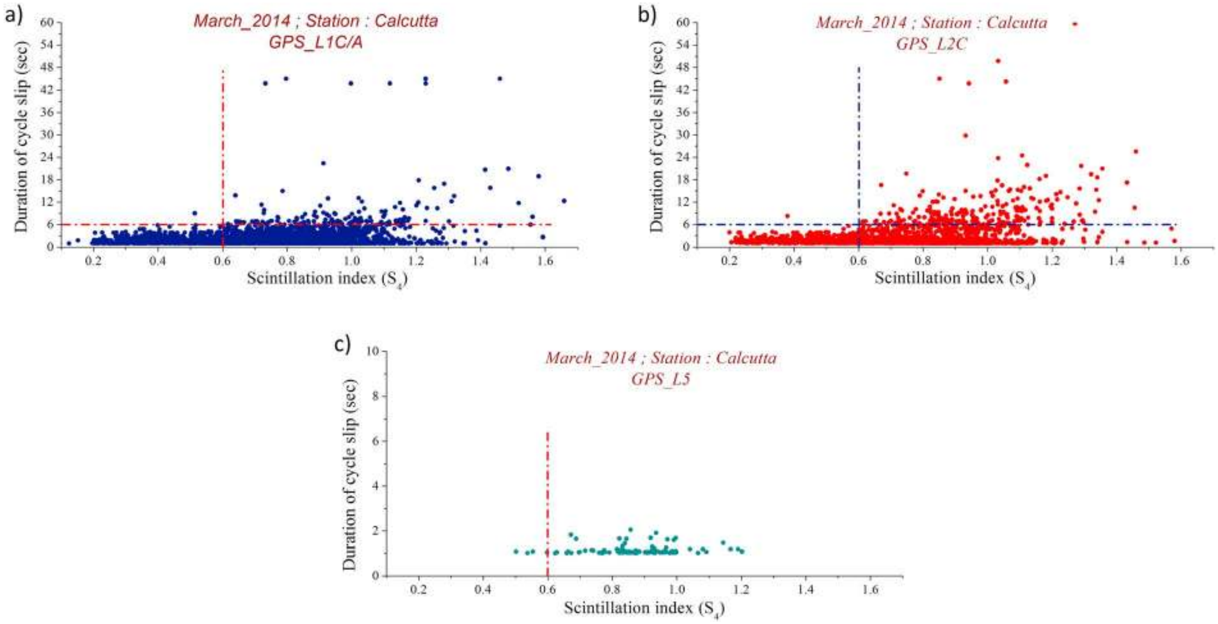

Figure 3. A correlation between intensity of amplitude scintillation index (S_4) and duration of cycle slips observed at (a) L1 C/A, (b) L2C, and (c) L5 of GPS during March 2014 from Calcutta. GPS = Global Positioning System.

In order to examine the relation between signal power and loss of lock events, duration of cycle slips ≥2 s has been plotted with respect to depth of signal fading during the periods of scintillations in Figures 4a and 4b for GPS L1 C/A and L2C, respectively, for the period of March 2014. As the number of cases of cycle slips of duration greater than 2 s is extremely small for L5, the analysis of depth of fading was not carried on at this frequency. It is observed from the figures, that for L2C, the depth of fading lie between 10 and 25 dB, whereas for L1 C/A, it varies over a wide range of 2–30 dB. However, the majority of the loss of lock events seem to occur for depth of fading values between 10 and 25 dB.

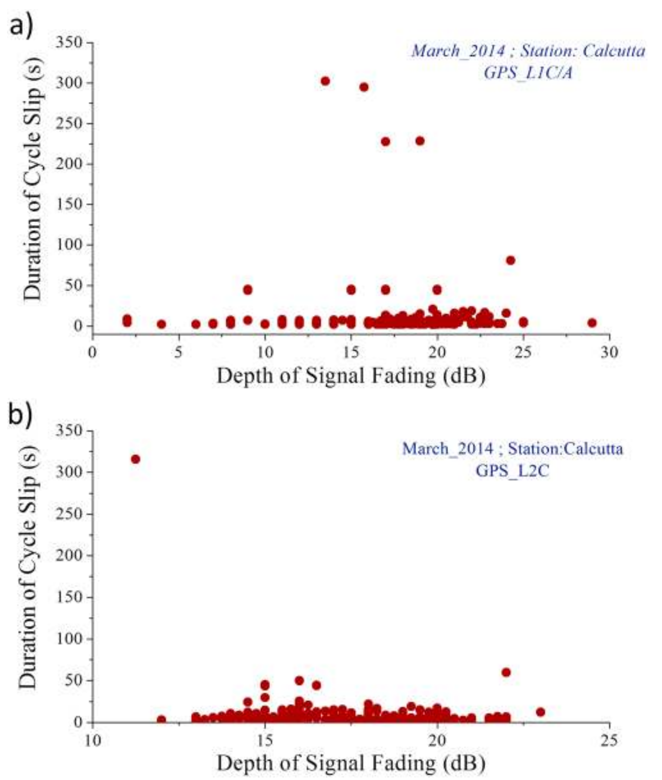

Figure 4. A relation between depths of signal fading and duration of cycle slip for March 2014 on all SVs at (a) GPS L1 C/A and (b) GPS L2C. GPS = Global Positioning System.

A case study of 18 February 2014 has been highlighted followed by the statistics of vernal equinox 2014. Figures 5a–5c show an enlarged section of detrended carrier phase plot of SV1 at GPS L1 C/A, L2C, and L5, respectively, on 18 February 2014. A close look at Figures 5a–5c clearly reveals an interesting result in terms of robustness of the triple-frequency GPS signals. In Figure 5a, loss of lock of 2.82 s is observed at GPS L1 C/A, which starts at 20:47 LT, while from Figure 5b, corresponding value of 6.52 s was observed at L2C around same time. Figure 5c shows, loss of lock of 1.50 s on GPS L5. Considering a case where loss of signal lock has started almost at the same time at all three GPS frequencies, it is clearly observed that duration of cycle slip is higher at L1 C/A than L5 and at L2C compared to L1 C/A, thereby indicating a less robustness of GPS L2C compared to other two signals L1 C/A and L5. Even though, the duration of cycle slips mentioned in the case study are not significant at L1 C/A and L5 as compared to ICAO specifications, duration of loss of lock at L2C is important.

In order to understand the correlation of cycle slips with amplitude scintillation index S_4 at different frequencies, Figures 6a–6c show the variation of S_4 with duration of cycle slip at GPS L1 C/A, L2C, and L5, respectively, as obtained from SV1 and SV24 during February–April 2014. In Figures 6a and 6c, the vertical lines at S_4 = 0.6 indicate that majority of loss of locks at GPS L1 C/A and L5 has been encountered for

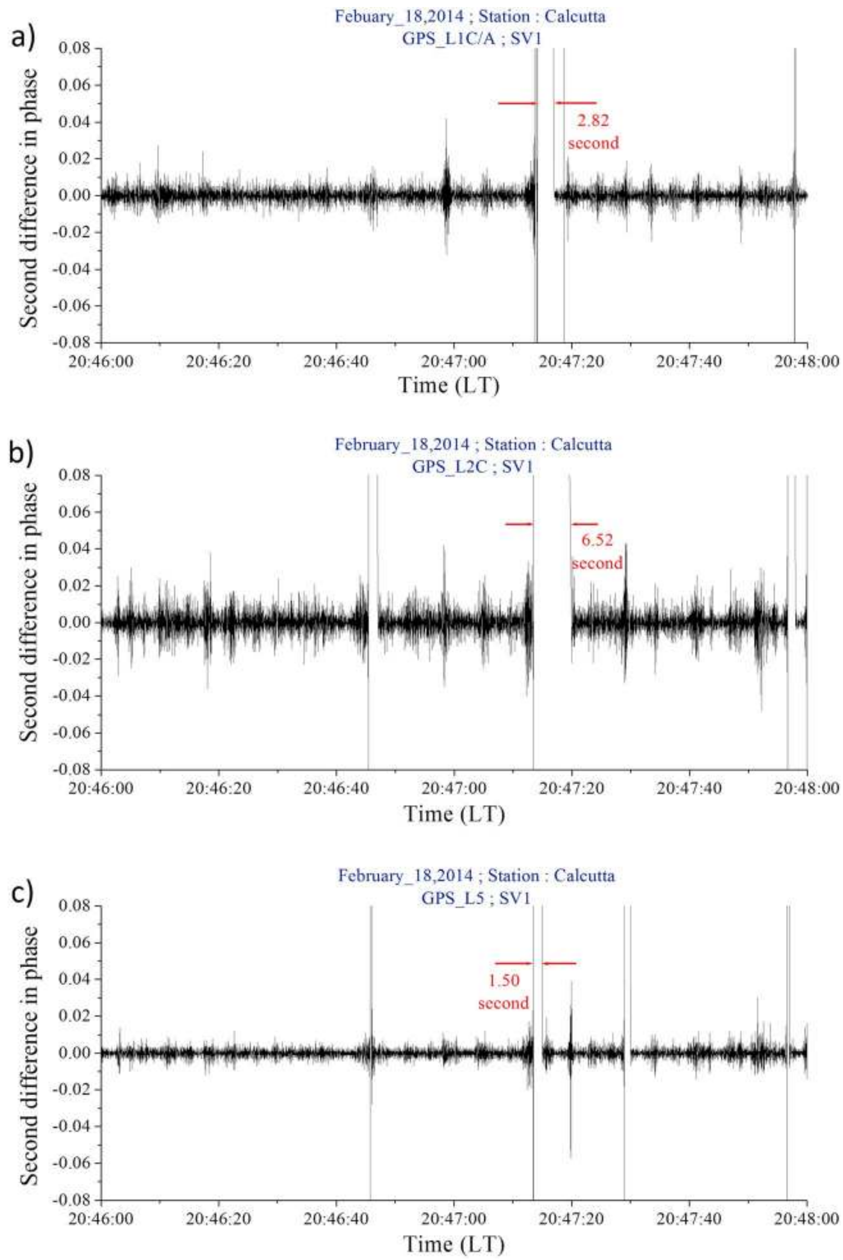

Figure 5. Case study of cycle slips observed on same SV link around same time interval at triple frequency of GPS on 18 February 2014. (a) Second difference in phase (cycles) at L1 C/A on SV1 during 20:46–20:48 LT. (b) Second difference in phase (cycles) at L2C on SV1 during 20:46–20:48 LT. (c) Second difference in phase (cycles) at L5 on SV1 during 20:46–20:48 LT. GPS = Global Positioning System.

$S_4 \geq 0.6$. Figure 6b presents a scenario, where along with large number of cases, durations of loss of lock greater than 6 s have been found mostly for $S_4 \geq 0.6$. This can be clearly noted from the position of the vertical and horizontal lines in Figure 6b. In addition to that, comparing the plots of Figures 6a–6c, it can also be observed that the number of cases of cycle slips detected at GPS L2C is higher than that at GPS L1 C/A and L5. Figure 6d shows the statistics of cycle slips occurring on GPS L1 C/A, L2C, and L5 in logarithmic scale, from Calcutta during vernal equinox of 2014 for SV1 and SV24. From the plot, it is found that number of cases of loss of locks affecting L2C is maximized having two cases of 8–10 s and four such cases of 6–8 s. For GPS L1 C/A no loss of lock is observed for duration greater than 6 s. Similarly for L5, maximum duration of cycle slip encountered is within 2–4 s. It is also important to

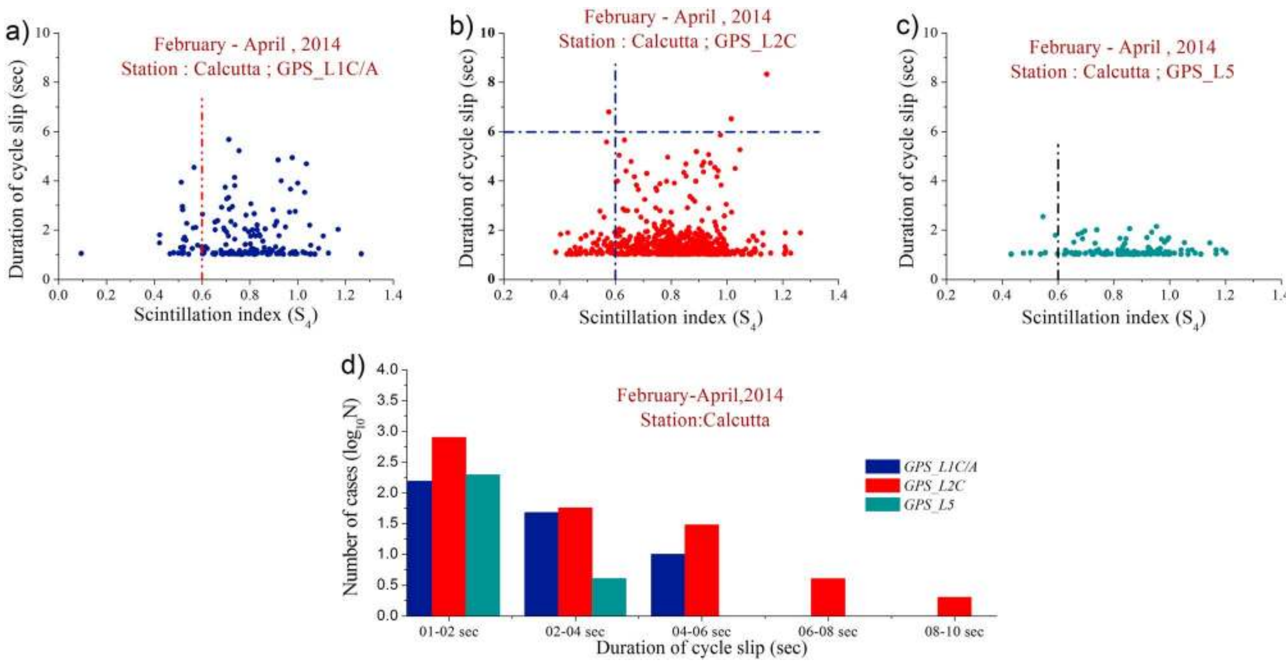

Figure 6. A correlation between intensity of amplitude scintillation index (S_4) and duration of cycle slips observed on same satellite links (SV1 and SV24) at (a) L1 C/A, (b) L2C, and (c) L5 of GPS during February–April 2014 from Calcutta. (d) A comparative statistical representation of number of cases of cycle slips in logarithmic scale, encountered on same satellite links (SV1 and SV24), respectively, at GPS L1 C/A, L2C, and L5 as a function of different time duration during February–April 2014. GPS = Global Positioning System.

notice from the plot that even though the majority of cycle slips took place for 1–2 s, occurrence is still highest for L2C than L1 C/A and L5. For durations of cycle slips greater than 2 s, it is observed that the three frequencies of GPS follow a pattern with duration of cycle slips at L2C > L1 C/A > L5. Considering the significance of loss of lock as specified by ICAO standards, these results lead to an important outcome that, of the three frequencies of GPS, GPS L5 is most robust while GPS L2C is least, under adverse ionospheric conditions.

4. Discussions

Space weather impacts on technology-based infrastructure could sometimes be as critical as life threatening under adverse ionospheric conditions especially for situations involving high dynamic platforms like an aircraft. Phase of a transionospheric satellite signal is an important tool to measure the outages of signals. Previously, events of cycle slips affecting GPS L1 and L2, from Calcutta and Siliguri near the northern crest of EIA, have been reported in literature (Roy & Paul, 2013).

The present paper, possibly reports for the first time, a comparative study from the perspective of loss of lock of triple-frequency GPS signals from a station Calcutta, located near the northern crest of the EIA in the Indian longitude sector during the present solar maxima. Durations of cycle slips observed in March 2014 at L1 C/A and L2C are significantly higher than the ICAO specified values for civil aviation. In addition, the occurrence of cycle slips is found to be more frequent and of longer durations at L2C during February–April 2014. Dependence of the intensity of amplitude scintillations on solar flux variations, specifically near the northern crest of EIA have previously been reported by Aarons (1982) indicating higher scintillation intensity during periods of high solar flux. The present analyses have found longer durations of loss of lock on GPS signals during February (monthly SSN: 146.1; F10.7 varies from 147.9 SFU to 188.1 SFU) than March (monthly SSN: 128.7; F10.7 varies from 134.2 SFU to 162.5 SFU) and April (monthly SSN: 112.5; F10.7 varies from 119.6 SFU to 185.2 SFU) depicting the effect of solar flux variation on the event, during the year 2014, which is consistent with Aarons (1982). The maximum value of loss of lock observed on SV1 at L2C is 8.32 s in February, while the corresponding values during March and April were 5.66 and 4.36 s, respectively. In an effort to correlate the loss of lock on the signal with intensity of amplitude scintillation, this work also reports the variation of S_4 with duration of cycle slip at all three GPS frequencies. From the analyses, it could be understood that majority of cycle slips occurred for S_4 values greater than 0.6 at all three frequencies of GPS (Figures 3 and 6a–6c). Along with that, the ICAO-mentioned safety time to alert 6 s is exceeded for $S_4 \geq 0.6$ (Figures 3a, 3b, and 6b). Jiao and Morton (2015) have found amplitude and phase scintillation events to be stronger and long lasting on L2C and L5 than on L1 C/A at both equatorial and high-latitude regions. Effects of ionospheric scintillations being inversely related with carrier frequencies, GPS L5 was expected to be most affected with longer durations of cycle slips than L2C. But the results of this exercise exhibit rather interesting outcome, where GPS L2C has experienced longer durations as well as more frequent cycle slips than L5.

Documents provided by (Aeronautical Radio, Incorporated, Engineering services, 2005, 2006a, 2006b) have illustrated GPS L5 to be substantially different from legacy L1 C/A or even the modernized L2C signals. The C/A code of GPS L1 signal is modulated with the Gold code and the L2C signal is a combination of C/A-, moderate length, and long length code on L2C (Hofmann-Wellenhof et al., 2008). Under the modernization program of GPS, the new GPS L5 has power specification, which is 3.6 to 4.5 dB stronger than L1 C/A (Hudnut & Titus, 2004). Another key aspect of GPS L5 is the implementation of Neuman Hoffman code, which reduces the narrowband interference effect and cross correlation, thereby providing more robust bit synchronization (van Dierendonck et al., 2000). Furthermore, the Quadrature-phase (Q5) and In-phase (I5) channels of the L5 signal are modulated with different PRN codes, which are completely orthogonal to each other. These codes are significantly different from C/A-, P-, and L2C codes used on L1 and L2 carriers both in terms of chipping rate and length. Natural chipping rate frequency of L1 and L2 signals is 10.23 MHz. For GPS L5, 10.23-megachip-per-second chipping rate was applied, which is 10 times that of C/A or L2C codes (Van Dierendonck & Hegarty, 2000). This enables L5 with a better rejection of narrowband in-band interference. Therefore, new GPS L5 is implemented with a pilot signal structure, such that it provides improved correlation properties, stronger signal power, and advanced interference protection (Hudnut & Titus, 2004). This might be a possible reason for better performance of the new GPS L5 in terms of signal tracking and consequently being less prone to cycle slip.

Seo et al. (2009) have defined deep fading in accordance with a particular receiver's carrier tracking loop performance, where deep fading is when a signal fade is deep enough to break the carrier tracking loop of the receiver. According to this definition, the value of the C/N_O dropping below a threshold value may lead to deep fades that may attribute to abrupt phase transition as mentioned by Humphreys et al. (2010). Jiao et al. (2015) have found deep signal fading events exceeding the threshold of −10 and −20 dB to be higher on L2C than L1 C/A and L5. Figures 4a and 4b of the present paper shows the variation of depth of signal fading during the events of loss of lock. Even though the values of depth of fading vary from 2–30 dB at L1 C/A, C/N_O value of a signal during the events of loss of lock were never found below 25 dB-Hz, which is the tracking range of the receiver in analysis.

Moraes, Vani, et al. (2018) have presented results where GPS L1 signal, have lower probabilities of being affected by moderate to strong scintillations compared to GPS L2C and L5 signal, which are in accordance with the inverse dependence of ionospheric scintillation intensity and carrier frequency. A fading model used by the above workers has verified the degraded performance of new L2C and L5 signals with respect to L1 signal. Jiao et al. (2016) reported L5 to have smaller tendency toward number of fades compared to L1 and L2C signal during the same period of scintillation and a decreased correlation between the GPS frequencies during strong scintillation. In the present work, effort has been made to compare L1 C/A signal with L2C and L5 signals in terms of loss of lock and cycle slips. The results of the analyses are explained in terms of the different codes used for modulation of the carrier frequencies to find L5 signal better in terms of performance during loss of lock events.

Delay et al. (2015) have previously reported the probability distribution of interrupted tracking of GPS L1, L2C, and L5 signals in terms of scintillation-induced data gap as a function of S_4 from a station near Brazil, thereby suggesting less robustness of L2C and L5 compared to L1. Decorrelation of GPS triple-frequency signals, in terms of S_4 and C/N_O, during periods of ionospheric scintillations, have been studied by Goswami et al. (2017) from Calcutta. Carrano et al. (2012) have also emphasized the use of frequency diversity to mitigate the effects of scintillation. They have also suggested that decorrelation of scintillation intensity with frequency enables the receiver to independently maintain lock on one of the tracking carriers. A study on GPS triple frequency from Brazil, in terms of amplitude and phase scintillation, has been presented by Moraes et al. (2017) where, variation of phase scintillation with local time and percentage concentration of the same with amplitude scintillation is shown as a function of frequency. A new approach was adopted by Vilà-Valls et al. (2017) to provide most reliable method of enhancing filtering performance in order to achieve robust tracking of the signal during severe scintillation events. These workers have established the new multivariate aggressive model to be superior in terms of robustness while considering cycle slip events.

Over time, several researchers have presented constructive results based on algorithms and simulations on cycle slip detection and repair mechanisms. Dai et al. (2009) have demonstrated an algorithm to detect and validate cycle slips for triple-frequency GPS receivers. Jiao and Morton (2015) have reported that a simulated signal with decreased decorrelation time is a threat to receiver processing and relative dynamics between GPS satellites and irregularities should be considered while developing robust receiver algorithms. The failure of the receiver to accurately detect and count an incoming signal leads to lost cycles. At this stage, a feasible solution as proposed by Lipp and Gu (1994) for repair of lost cycles could be arrived at by utilizing the short-term stability of an Inertial Navigation System. Humphreys et al. (2005) evaluated the performance of several GPS carrier tracking loops in order to examine the PLL structure that enable good phase tracking during power fades induced by strong equatorial scintillation. Their experimental outcome indicate that constant bandwidth PLLs (~15 Hz) tend to lose phase lock during scintillations compared to the decision-directed discriminator, which reduces the carrier lock threshold by ~1 dB. So far, different models have been developed for studying scintillation effects on PLLs. But these models are somewhat inadequate for scintillations, frequently encountered at equatorial and low latitudes.

5. Conclusion

Space Weather broadly refers to the Earth-Sun environment, which may affect systems operating within this region. Intense Space Weather events in Earth's ionosphere may cause complete outage of transionospheric satellite signals, thereby posing severe threat to the satellite-based communication and navigation systems.

Calcutta being situated near the northern crest of EIA is severely prone to outage of signals during intense scintillations occurring over the magnetic equator (Paul et al., 2011). Considering this fact, some interesting results have been found when comparing the modernized GPS signals L2C and L5 with the legacy L1 C/A signal from station. The effect of adverse ionospheric conditions on lower-frequency carrier being more intense due to inverse dependence of scintillation on frequency, GPS L5 was expected to be most affected by events of signal outages during ionospheric scintillations. But statistical outcome from the data analyzed during the vernal equinox of 2014 suggest the fact that occurrence of loss of lock is more frequent at L2C than L1 C/A and L5. Previously, Jiao et al. (2016) have found L5 to have smaller tendency toward signal fades compared to L1 and L2C signals considering same period of scintillations. Results of present study also suggest that relative robustness of the three GPS signals in terms of occurrence and durations of cycle slips could follow the sequence L5 > L1 C/A > L2C, thereby defining the modernized GPS L5 as most robust and GPS L2C as least robust for signal tracking.

High-latitude ionosphere is dominated by phase scintillation events over amplitude scintillations caused by the ionospheric density gradients and precipitation of electrons along the geomagnetic field lines (Prikryl et al., 2014). Jiao and Morton (2015) have reported observations made from Gakona, Alaska (62.4°N, 145.2°W geographic); Jicamarca, Peru (11.9°S, 76.9°W geographic); and Ascension Island (7.9°S, 14.4°W geographic), which shows that scintillation events at high latitudes are more likely to occur when A_P/K_P index is higher but equatorial scintillations are mostly independent of geomagnetic activity. They have also found that equatorial scintillation is more severe and long lasting than that at high-latitude region. The present paper reports analyses from equatorial station Calcutta (22.58°N, 88.38°E geographic; magnetic dip 32°N) during geomagnetic quiet period (*Dst* index ≤ -50 nT; $K_p < 5$) and finds cases of intense amplitude scintillations ($S_4 \geq 0.6$) that are correlated with loss of lock events at triple frequency of GPS. Loss of locks associated with intense scintillations observed from this station under geomagnetic quiet period are results that are in accordance with Jiao and Morton (2015). However, this paper also finds the events of loss of lock due to ionospheric scintillations to be maximum at L2C and minimum at L5, which is different from Jiao and Morton (2015) who found scintillation events on both L2C and L5 to be higher than L1 C/A at high and low latitudes as well.

Chen et al. (2008) reported a 3-year (2001–2003) study from Hong Kong (22°N geographic, 12°N geomagnetic). Results obtained from this equatorial station show that, during geomagnetic quiet period, loss-of-lock events are mostly encountered for L2 compared to L1 frequency. The results obtained for the present analyses during geomagnetic quiet conditions corroborate the findings of Chen et al. (2008).

Durations of loss of lock events, found on GPS L1 C/A and L2C signals, are above the threshold values mentioned by the ICAO for civil aviation operation, which is 6 s for APV-I and 10 s for APV-II. However, GPS L5 adheres to ICAO APV specifications encountering no such high values of cycle slip durations, thereby justifying the robustness of the signal.

Probability of signal fades up to a particular level can be directly related to the S_4 index (Delay et al., 2015). Therefore, when the signal level drops below a certain threshold, the receiver becomes prone to loss of lock, which varies as a function of S_4 index (Carrano & Groves, 2010). Therefore, in an effort to correlate occurrence of cycle slip events with intensity of amplitude scintillation, the present study has observed that occurrence of loss of lock and cycle slips for all three GPS frequencies are more frequent when $S_4 \geq 0.6$. It is also important to note that majority of cycle slips of duration more than 6 s are found for $S_4 \geq 0.6$.

Data analyzed from the Canadian High Arctic Ionospheric Network shows that number of cases of cycle slips, caused mainly by auroral arcs that are high prior to local magnetic midnight (Prikryl et al., 2010). The present paper shows hourly variation of loss of lock events observed at GPS L1 C/A from equatorial station Calcutta. The events of loss of lock are found to be large in number, and their occurrence is correlated with $S_4 \geq 0.6$ even after local midnight.

Acknowledgments
This research has been sponsored in part by the Centre of Advanced Studies in Radio Physics and Electronics at University of Calcutta. One of the authors (T. B.) acknowledges the support provided by Council of Scientific and Industrial Research (CSIR), Government of India, at Institute of Radio Physics and Electronics (IRPE), University of Calcutta, in the form of a fellowship. Authors are thankful to Kyoto University for providing geomagnetic data on the website wdc.kugi.kyoto-u.ac.jp/dstdir/. The processed data used for this study have been uploaded for sharing among the community as suggested. The corresponding doi assigned to the dataset is 10.5281/zenodo.2613523.

References

Aarons, J. (1982). Global morphology of ionospheric scintillations. *Proceedings of the IEEE*, *70*(4), 360–378.

Anderson, D. N., & Haerendel, G. (1979). The motion of depleted plasma regions in the equatorial ionosphere. *Journal of Geophysical Research*, *84*(A8), 4251–4256.

ARINC Engineering Services (2005). NAVSTAR GPS space segment/user segment L5 interfaces, *Interface specification,* IS-GPS-705, IRN-705-003, www.arinc.com/gps

ARINC Engineering Services (2006a). NAVSTAR GPS space segment/navigation user interfaces, *Interface specification*, IS-GPS-200, revision D, IRN-200D-001, www.arinc.com/gps

ARINC Engineering Services (2006b). NAVSTAR GPS space segment/user segment L1C interfaces, *Interface specification*, Draft IS-GPS-800, www.navcen.uscg.gov/gps/modernization

Basu, S., Basu, S., Huba, J., Krall, J., McDonald, S. E., Makela, J. J., et al. (2009). Day-to-day variability of the equatorial ionization anomaly and scintillations at dusk observed by GUVI and modeling by SAMI3. *Journal of Geophysical Research*, *114*, A04302. https://doi.org/10.1029/2008JA013899

Bhattacharyya, A., Groves, K. M., Basu, S., Kuenzler, H., Valladares, C. E., & Sheehan, R. (2003). L-band scintillation activity and space-time structure of low-latitude UHF scintillations. *Radio Science*, *38*(1), 1004. https://doi.org/10.1029/2002RS002711

Carrano, C. S., & Groves, K. M. (2010). 23rd International Technical Meeting of the satellite Division of The Institute of Navigation, Portland OR, September 21-24,.

Carrano, C. S., Groves, K. M., McNeil, W. J., & Doherty, P. H. (2012). Scintillation Characteristics across the GPS Frequency Band, 25th International Technical Meeting of the Satellite Division of The Institute of Navigation, Nashville TN, September 17-21.

Chen, W., Gao, S., Hu, C., Chen, Y., & Ding, X. (2008). Effects of ionospheric disturbances on GPS observation in low latitude area. *GPS Solutions*, *12*(1), 33–41.

Dai, Z., Knedlik, S., & Loffeld, O. (2009). Instantaneous triple-frequency GPS cycle slip detection and repair. *International Journal of Navigation and Observation*, *2009*, 1–15. https://doi.org/10.1155/2009/407231

Das, A., Gupta, A. D., & Ray, S. (2010). Characteristics of L-band (1.5 GHz) and VHF (244 MHz) amplitude scintillations recorded at Kolkata during 1996–2006 and development of models for the occurrence probability of scintillations using neural network. *Journal of Atmospheric and Solar-Terrestrial Physics*, *72*(9-10), 685–704.

DasGupta, A., Paul, A., Ray, S., Das, A., & Ananthakrishnan, S. (2006). Equatorial bubbles as observed with GPS measurements over Pune, India. *Radio Science*, *41*, RS5S28. https://doi.org/10.1029/2005RS003359

Delay, S. H., Carrano, C., Groves, K., & Doherty, P. H. (2015). A statistical analysis of GPS L1, L2 and L5 tracking performance during ionospheric scintillation. Proc. 2015 ION Pacific PN T Conference, Honolulu, Hawaii, April 20-23, 1-8.

Goswami, S., Paul, A., & Haldar, S. (2018). Study of relative performance of different navigational satellite constellations under adverse ionospheric conditions. *Space Weather*, *16*, 667–675. https://doi.org/10.1029/2017SW001762

Goswami, S., Paul, K. S., & Paul, A. (2017). Assessment of GPS multifrequency signal characteristics during periods of ionospheric scintillations from an anomaly crest location. *Radio Science*, *52*, 1214–1222. https://doi.org/10.1002/2017RS006295

Hofmann-Wellenhof, B., Lichtenegger, H., & Wasle, E. (2008). *GNSS—Global Navigation Satellite Systems: GPS, GLONASS, Galileo, and more*. Berlin, Germany: Springer Science & Business Media.

Hudnut, K. W., & Titus, B. (2004). GPS L1 civil signal modernization (L1C), The Interagency GPS Executive Board, www.navcen.uscg.gov/gps

Humphreys, T. E., Psiaki, M. L., & Kintner, P. M. Jr. (2005). GPS carrier tracking loop performance in the presence of ionospheric scintillations. *Proc.* 2005 *ION GNSS Conference,* Long Beach, CA, September 13-16.

Humphreys, T. E., Psiaki, M. L., & Kintner, P. M. Jr. (2010). Modeling the effects of ionospheric scintillation on GPS carrier phase tracking. *IEEE Transactions on Aerospace and Electronic Systems*, *46*(4), 1624–1637. https://doi.org/10.1109/TAES.2010.5595583
International Civil Aviation Organization. Manual on air traffic forecasting. Vol. 8991. ICAO, 2006.
Jiao, Y., & Morton, Y. T. (2015). Comparison of the effect of high-latitude and equatorial ionospheric scintillation on GPS signals during the maximum of solar cycle 24. *Radio Science*, *50*, 886–903. https://doi.org/10.1002/2015RS005719
Jiao, Y., Morton, Y. T., Akos, D., & Walter, T. (2015). A comparative study of triple frequency GPS scintillation signal amplitude fading characteristics at low latitudes. In Proc. 28th Int. Tech. Meet. The Satellite Division Inst. Navig. (pp. 3819-3825).
Jiao, Y., Rino, C., & Morton, Y. T. (2018). Ionospheric scintillation simulation on equatorial GPS signals for dynamic platforms. *Navigation: Journal of The Institute of Navigation*, *65*(2), 263–274.
Jiao, Y., Xu, D., Morton, Y., & Rino, C. (2016). Equatorial scintillation amplitude fading characteristics across the GPS frequency bands. *Navigation*, *63*(3), 283–294. https://doi.org/10.1002/navi.146
Kelley, M. C., Haerendal, G., Kappler, H., Valenzuela, A., Balsley, B. B., Carter, D. A., et al. (1976). Evidence for a Rayleigh-Taylor type instability and upwelling of depleted density regions during equatorial spread-*F*. *Geophysical Research Letters*, *3*, 448–450. https://doi.org/10.1029/GL003i008p00448
Kintner, P. M., Kil, H., Beach, T. L., & de Paula, E. R. (2001). Fading timescales associated with GPS signals and potential consequences. *Radio Science*, *36*(4), 731–743. https://doi.org/10.1029/1999RS002310
Kintner, P. M., Ledvina, B. M., de Paula, E. R., & Kantor, I. J. (2004). Size, shape, orientation, speed, and duration of GPS equatorial anomaly scintillations. *Radio Science*, *39*, RS2012. https://doi.org/10.1029/2003RS002878
Lipp, A., & Gu, X. (1994). Cycle slip detection and repair in integrated navigation systems, *Proceedings of* 1994 *IEEE Position, Location and Navigation Symposium PLANS 94*, Las Vegas, NV, USA, 1994, 681-688. https://doi.org/10.1109/PLANS.1994.303377
Liu, Z. (2010). A new automated cycle slip detection and repair method for a single dual-frequency GPS receiver. *Journal of Geodesy*, *85*(3), 171–183. https://doi.org/10.1007/s00190-010-0426-y
McClure, J. P., Hanson, W. B., & Hoffman, J. H. (1977). Plasma bubbles and irregularities in the equatorial ionosphere. *Journal of Geophysical Research*, *82*, 2650–2656. https://doi.org/10.1029/JA082i019p02650
Moraes, A., Costa, E., Abdu, M. A., Rodrigues, F. S., de Paula, E. R., Oliveira, K., & Perrella, W. J. (2017). The variability of low-latitude ionospheric amplitude and phase scintillation detected by a triple-frequency GPS receiver. *Radio Science*, *52*, 439–460. https://doi.org/10.1002/2016RS006165
Moraes, A. O., Muella, M. T. A., de Paula, E. R., de Oliveira, C. B. A., Terra, W. P., Perrella, W. J., & Meibach-Rosa, P. R. P. (2018). Statistical evaluation of GLONASS amplitude scintillation over low latitudes in the Brazilian territory. *Advances in Space Research*, *61*(7), 1776–1789. https://doi.org/10.1016/j.asr.2017.09.032
Moraes, A. O., Rodrigues, F. S., Perrella, W. J., & de Paula, E. R. (2011). Analysis of the characteristics of low-latitude GPS amplitude scintillation measured during solar maximum conditions and implications for receiver performance. *Surveys in Geophysics*, *33*(5), 1107–1131. https://doi.org/10.1007/s10712-011-9161-z
Moraes, A. O., Vani, B. C., Costa, E., Sousasantos, J., Abdu, M. A., Rodrigues, F., et al. (2018). Ionospheric scintillation fading coefficients for the GPS L1, L2, and L5 frequencies. *Radio Science*, *53*, 1165–1174. https://doi.org/10.1029/2018RS006653
Paul, A., & DasGupta, A. (2010). Characteristics of the equatorial ionization anomaly in relation to the day-to-day variability of ionospheric irregularities around the postsunset period. *Radio Science*, *45*, RS6001. https://doi.org/10.1029/2009RS004329
Paul, A., Paul, K. S., & Das, A. (2017). Impact of multi-constellation satellite signal reception on performance of satellite-based navigation under adverse ionospheric conditions. *Radio Science*, *52*, 416–427. https://doi.org/10.1002/2016RS006076
Paul, A., Roy, B., Ray, S., Das, A., & DasGupta, A. (2011). Characteristics of intense space weather events as observed from a low latitude station during solar minimum. *Journal of Geophysical Research*, *116*, A10307. https://doi.org/10.1029/2010JA016330
Prikryl, P., Jayachandran, P. T., Mushini, S. C., Pokhotelov, D., MacDougall, J. W., Donovan, E., et al. (2010). GPS TEC, scintillation and cycle slips observed at high latitudes during solar minimum. *Annales Geophysicae* (09927689), *28*(6), 1307–1316.
Prikryl, P., Jayachandran, P. T., Mushini, S. C., & Richardson, I. G. (2014). High-latitude GPS phase scintillation and cycle slips during high-speed solar wind streams and interplanetary coronal mass ejections: A superposed epoch analysis. *Earth, Planets and Space*, *66*(1), 62.
Rastogi, R. G., & Klobuchar, J. A. (1990). Ionospheric electron content within the equatorial F2 layer anomaly belt. *Journal of Geophysical Research*, *95*(A11), 19,045–19,052.
Ray, S., & DasGupta, A. (2007). Geostationary L-band signal scintillation observations near the crest of equatorial anomaly in the Indian zone. *Journal of Atmospheric and Solar - Terrestrial Physics*, *69*(4-5), 500–514.
Roy, B., & Paul, A. (2013). Impact of space weather events on satellite-based navigation. *Space Weather*, *11*, 680–686. https://doi.org/10.1002/2013SW001001
RTCA (2006). Minimum operational performance standards for Global Positioning System/Wide area augmentation system airborne equipment, RTCA DO-229D, 13 Dec.
Seo, J., Walter, T., Chiou, T.-Y., & Enge, P. (2009). Characteristics of deep GPS signal fading due to ionospheric scintillation for aviation receiver design. *Radio Science*, *44*, RS0A16. https://doi.org/10.1029/2008RS004077
Singleton, D. G. (1970). The effect of irregularity shape on radio star and satellite scintillations. *Journal of Atmospheric and Solar - Terrestrial Physics*, *32*(3), 315–343.
Van Dierendonck, A. J., & Hegarty, C. (2000). The new L5 civil GPS signal. *GPS World*, *11*(9), 64–71.
van Dierendonck, A. J., Hegarty, C., Scales, W., & Ericson, S. (2000). Signal specification for the future GPS civil signal at L5, *Presented at the IAIN World Congress, San Diego*, California, June 27.
Vilà-Valls, J., Closas, P., & Curran, J. T. (2017). Multi-frequency GNSS robust carrier tracking for ionospheric scintillation mitigation. *Journal of Space Weather and Space Climate*, *7*, A26. https://doi.org/10.1051/swsc/2017020